REPORT NO. NAS9-4770-TR2

NASA CR. 151824

PSEUDO NOISE TESTING

TECHNICAL REPORT
CONTRACT NAS9-14770

SUBMITTED TO:

NATIONAL AERONAUTICS AND SPACE ADMINISTRATION
LYNDON B. JOHNSON SPACE CENTER
HOUSTON, TEXAS

JUNE 30, 1978

ALABAMA AGRICULTURAL AND MECHANICAL UNIVERSITY
SCHOOL OF TECHNOLOGY
HUNTSVILLE, ALABAMA

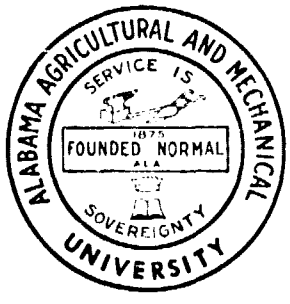

Report No. NAS9-14770-TR2

PSEUDO NOISE TESTING

Technical Report
Contract NAS9-14770
Supplement 2S

Submitted To

National Aeronautics And Space Administration
Lyndon B. Johnson Space Center
Houston, Texas

Submitted By

School of Technology
Alabama A&M University
Normal, Alabama

June 30, 1978

PSEUDO NOISE TESTING

1. INTRODUCTION

This document is a technical report covering effort under contract NAS9-14770, Supplement 2S for the period March 1, 1977 to June 30, 1978. The report is divided into three parts describing the three tasks covered under Supplement 2S. These tasks include:

(1) A study of the application of pseudo noise testing.

(2) A modification of the PN Test Set to include the capability of digital filtering in the data and reference channels.

(3) A study of a synthesis procedure for long PCM frame synchronization words.

RMS distortion, as measured by the Pseudo Noise Test Set, can be used to establish a quality factor for the transmission of data-like analog signals through a communications channel. The test set performs an evaluation of channel performance based upon its ability to compare a system output with a time-delayed version of the system input. This report describes an investigation into the utility of the test set measurements in several applications. The approach was to provide an analysis of the expected results under particular channel conditions.

Under the contract, the PN Test Set was modified to include digital filters for the data and reference channels. These units can be used as an alternative to the matched analog filters in the origional design, and they provide a certain degree of flexibility not previously available in utilizing the test set. The test set design modifications necessary to implement the digital filters are described in Section 3.

A study of an algorithm for the identification of long PCM frame synchronization words with desirable non-periodic autocorrelation properties is described in Section 4.

2. APPLICATION OF PSEUDO NOISE TESTING

2.1 Comparison of Channel RMS Distortion and Channel Capacity Loss

This section is an analysis which compares RMS distortion, as measured by the Pseudo Noise Test Set, to channel capacity loss in passing a complex data signal through a communications channel. This study was performed in order to provide a better basis for comparing RMS distortion measured using pseudo randon noise and other parameters available for the specification of communications channel quality.

The approach taken was to assume a data source with a signal power spectral density shown in Figure 1. The communications channel was assumed to consist of an additive white noise source and an ideal "brick-wall" response low-pass filter as shown in Figure 2. The resulting channel output is shown in figure 3.

The shape of the data spectrum was selected because it approximates a realistic signal spectrum, and because this selection allows a reduction in the complexity of the analysis.

Two parameters were calculated, the reduction in the information carying ability of the channel output waveform as compared to the channel filter input waveform, and the RMS distortion resulting when the signal passes through the channel.

The potential information content of a signal is

$$I = \int_0^{f_d} \log_2(1 + S(f)/N(f))df$$

where S(f) is the signal spectral density, and N(f) is the noise spectral density. The ratio of the potential information content of the signal before and after the channel

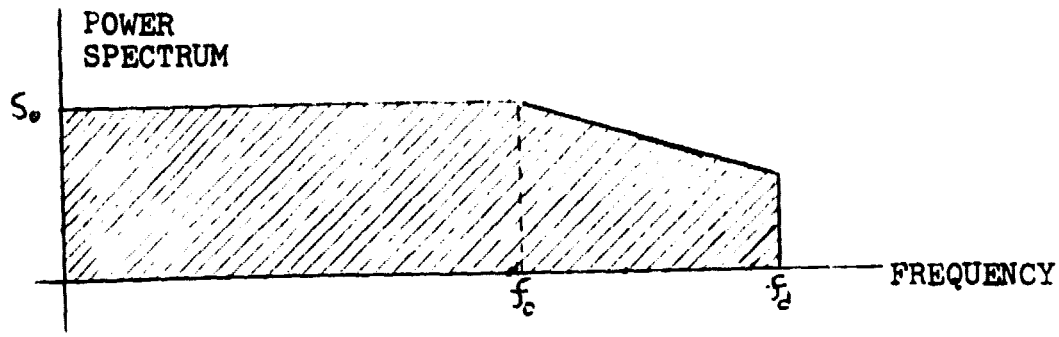

Figure 1 Assumed Data Source Power Spectrum

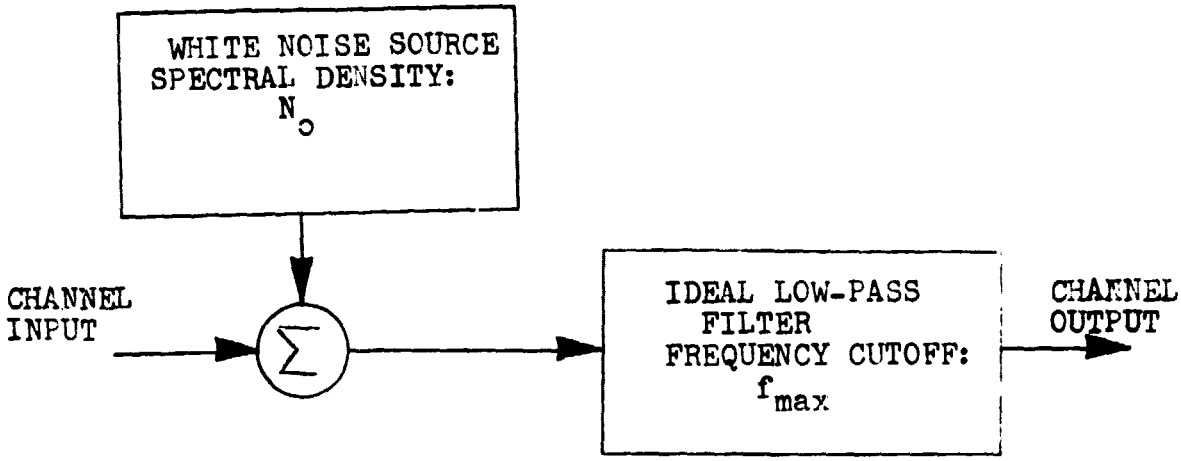

Figure 2 Assumed Channel Model

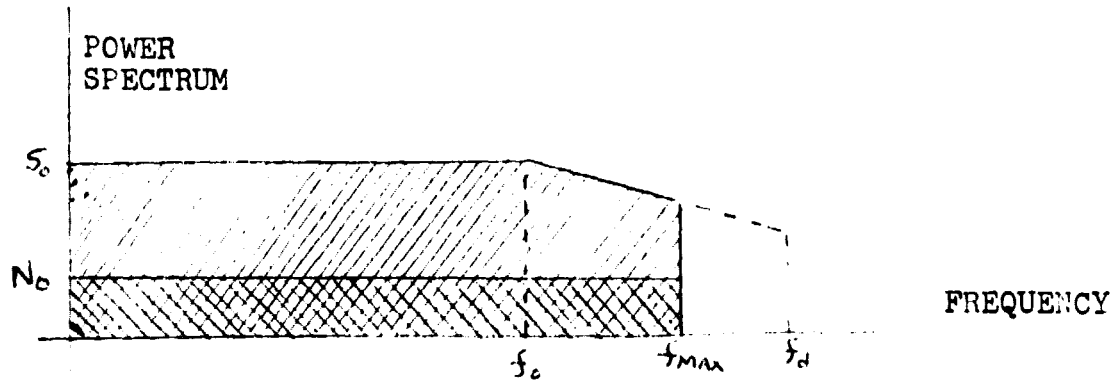

Figure 3 Channel Output Signal and Noise Power Spectrum

filter is given by the expression

$$R = \frac{((f_d - f_{max})/f_o)\ln(S_o/N_o - 2nR_1}{(f_d/f_o)\ln(f_d/f_o) - 2nR_2}$$

where

$$R_1 = (f_d/f_o)\ln(f_d/f_o) - (f_{max}/f_o)\ln(f_{max}/f_o) - (f_d - f_{max})/f_o$$

$$R_2 = (f_d/f_o)\ln(f_d/f_o) - f_d/f_o + 1$$

and

$$S_o/N_o \gg (f_{max}/f_o)^{2n}$$

The order of the data is n, where $S_o(f_o/f)^{2n}$ is the spectral density in the roll-off portion of the signal spectrum.

The RMS distortion for the data spectrum passing through the channel is

$$E = \frac{(1/(2n-1))E_1 + (1/(S_o/N_o))(f_{max}/f_o)}{1 + (1/(2n-1))(1-(f_o/f_d)^{2n-1})}$$

where

$$E_1 = (f_o/f_{max})^{2n-1} - (f_o/f_d)^{2n-1}$$

E and R were calculated for several cases, and the results are given in Figures 4, 5, and 6.

The results show that the channel capacity loss percentage and the RMS distortion percentage both monotonically decrease with increasing channel bandwidth up to the f_d limit. Also, if the data characteristics are known a priori, and a given percentage loss in potential channel capacity can be tolerated, the verification of proper operation of the channel can be accomplished by measuring RMS distortion and comparing this value of E to the expected value for the allowed value of R.

2.2 Spectral Properties of the PN Test Set Error Spectrum

This section presents the results of a study of the spectral properties of the error output signal of the PN Test Set. It has been observed that for low-pass data transfered through a low-pass channel, the spectrum of the error output signal (RMS mismatch), when the error signal is minimized, is shown in Figure 7. The peak of the spectral density curves occurs slightly beyond the cutoff (-3db) frequency of the channel.

The objective of the study was to better understand the utility of the end-to-end RMS distortion measurement as a means of communications system evaluation. The approach was to develop a mathematical model of the error signal forming process in the frequency domain.

Figures 8 and 9 illustrate the PN test-set data spectrum, the communications system bandpass characteristics, and the PN test-set output spectrum. The mathematical models of the spectra of figure 9 are:

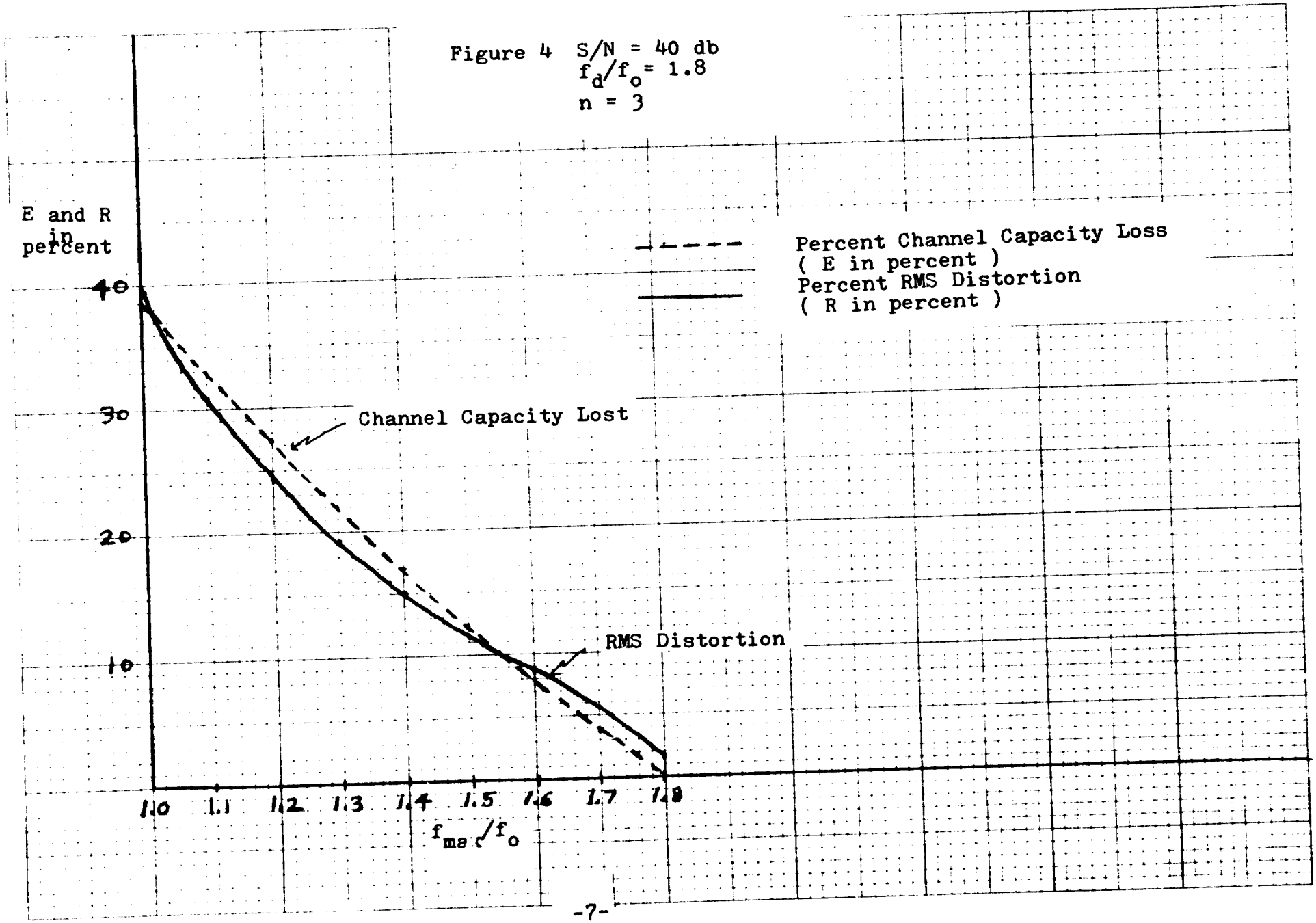

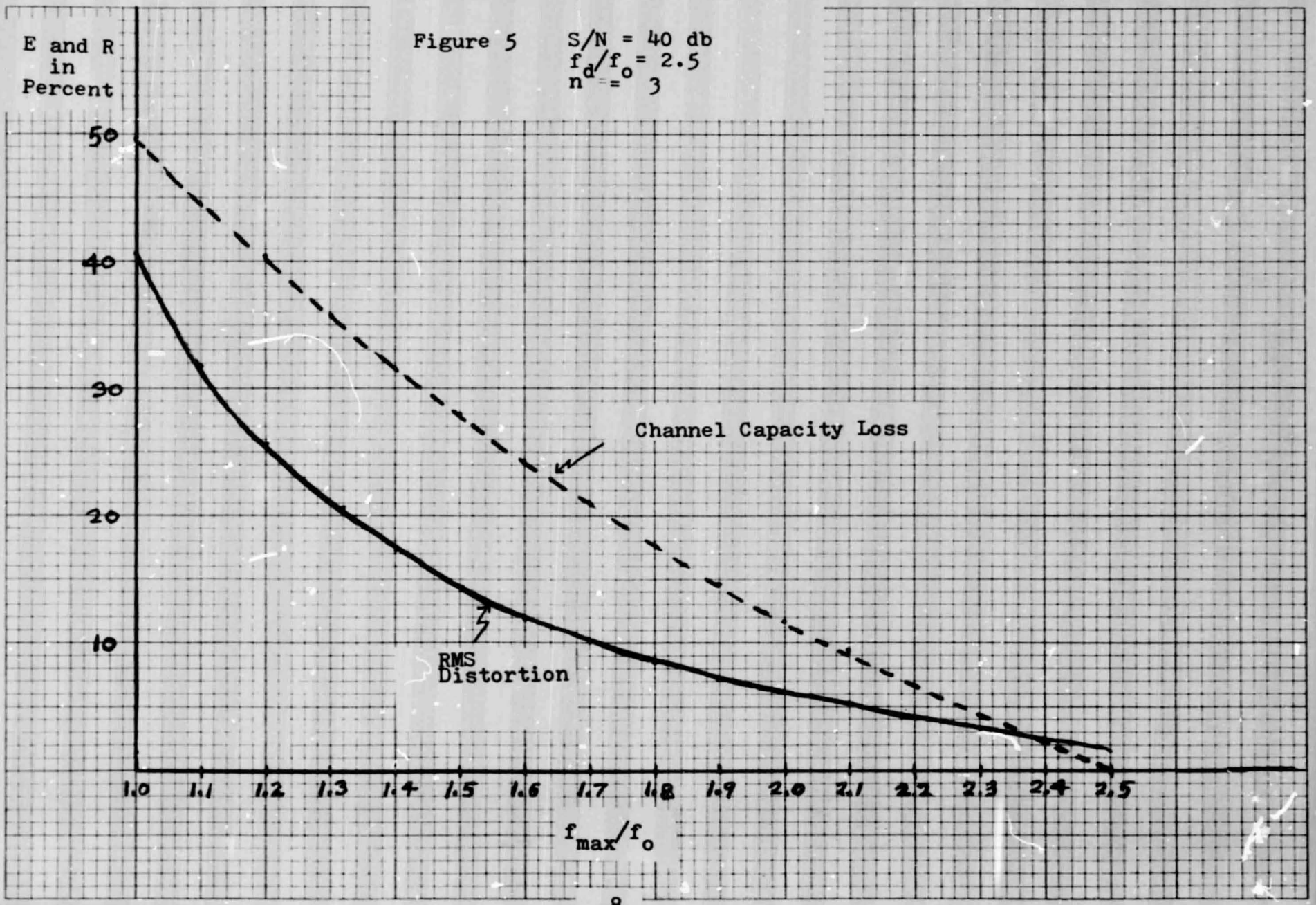

Figure 5 $S/N = 40$ db
$f_d/f_o = 2.5$
$n = 3$

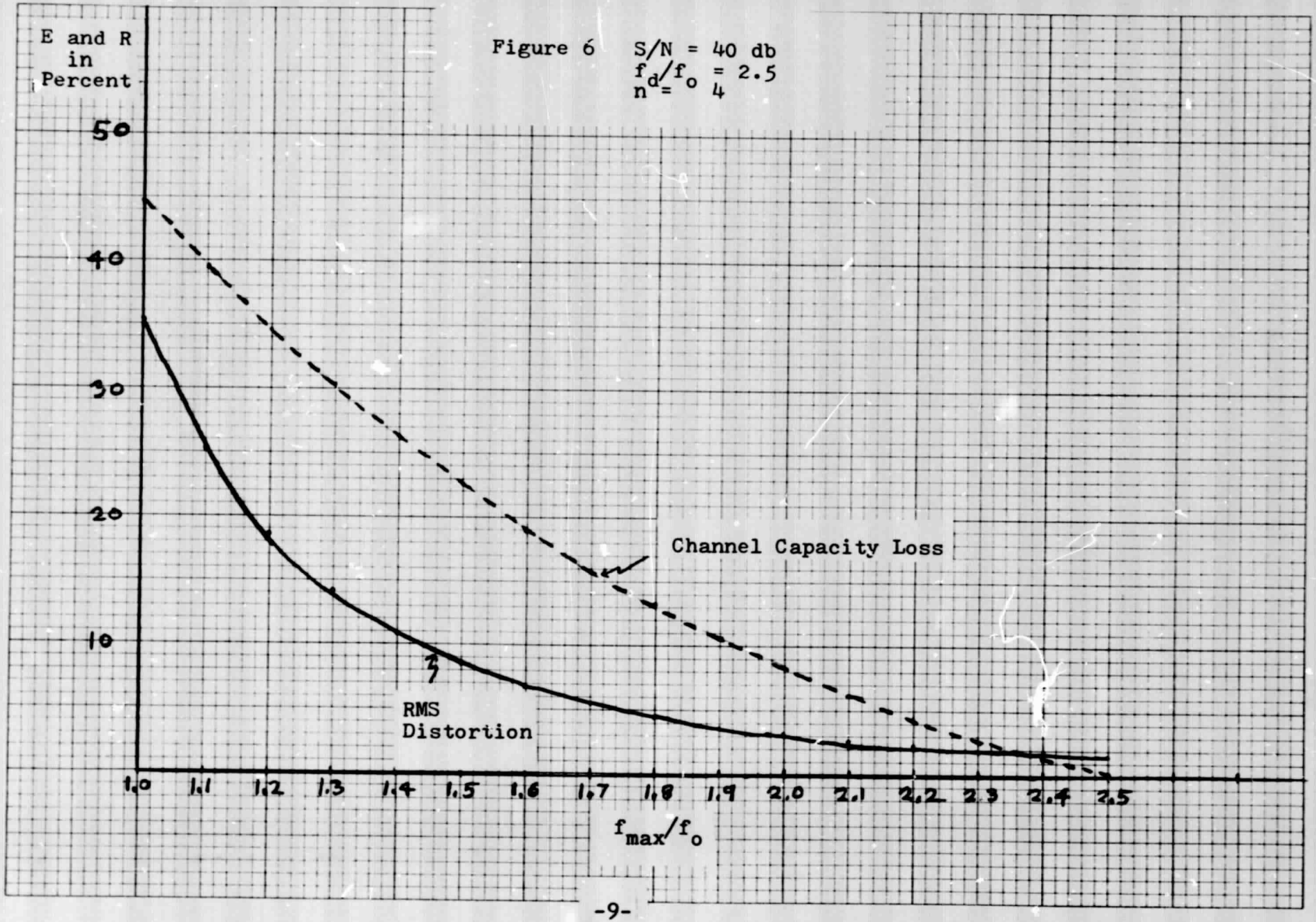

Figure 6 S/N = 40 db
f_d/f_o = 2.5
n = 4

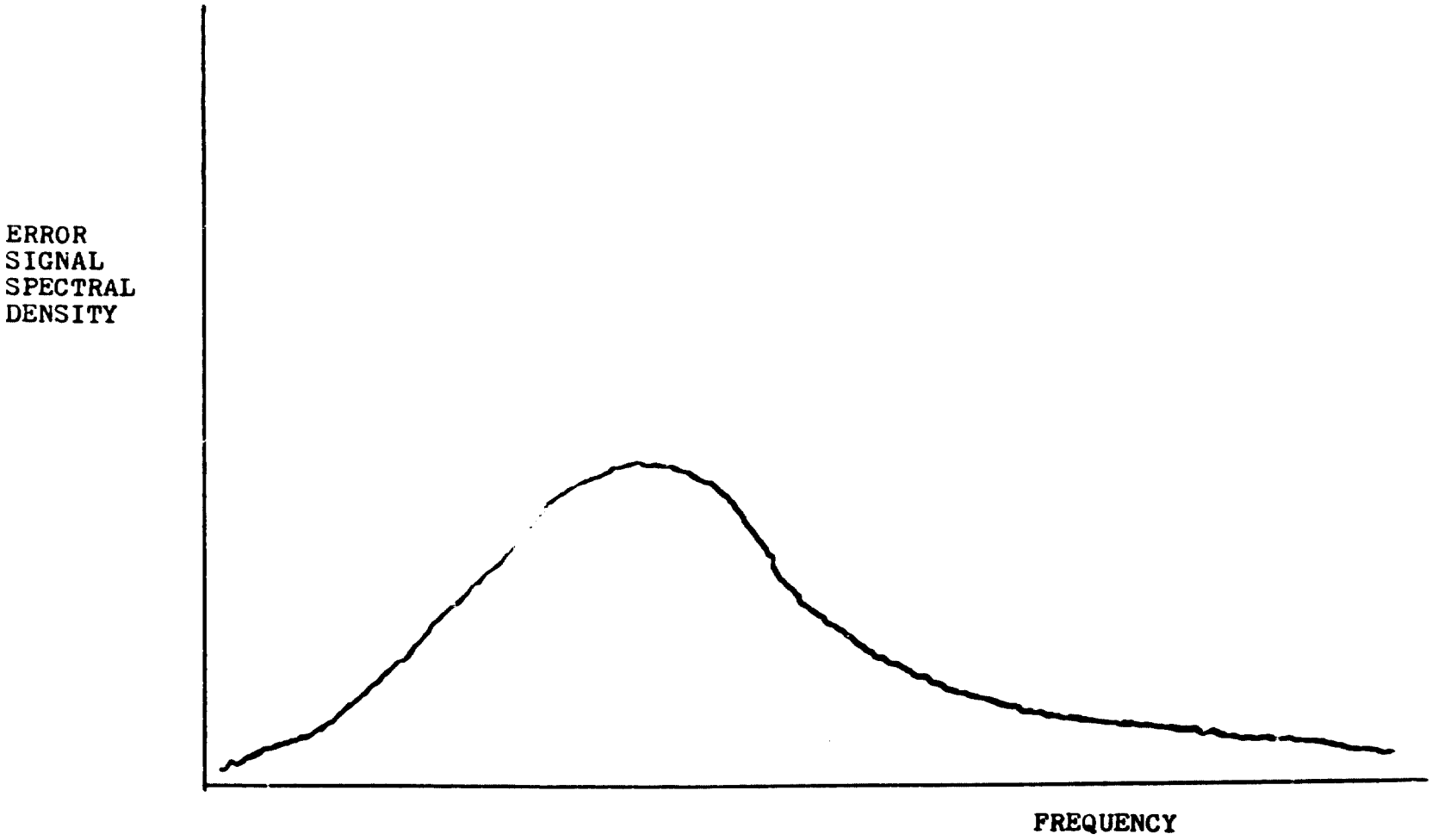

Figure 7 Observed PN Test Set Error Spectrum

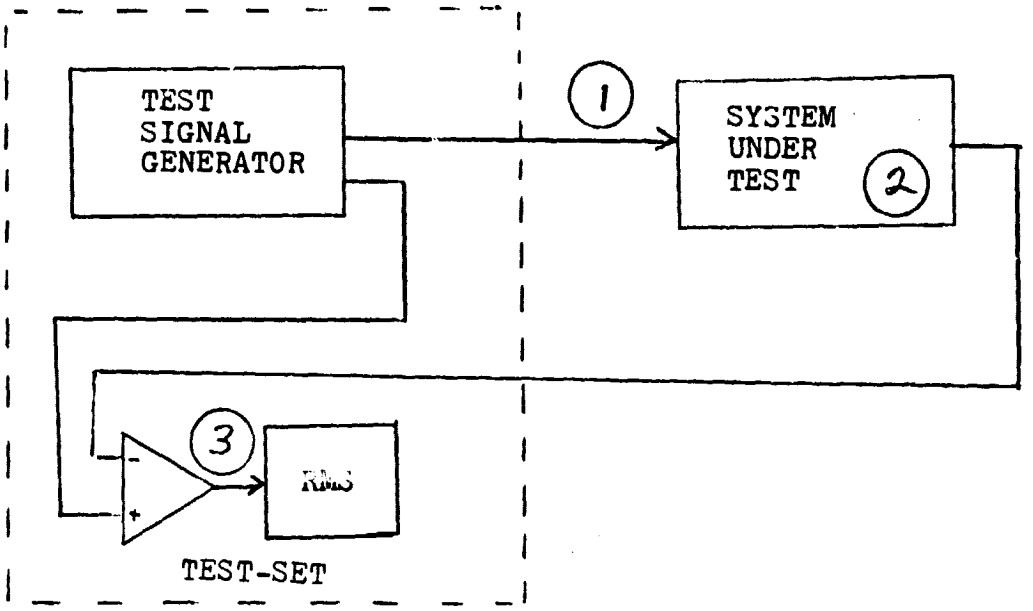

Figure 8 PN Test Block Diagram

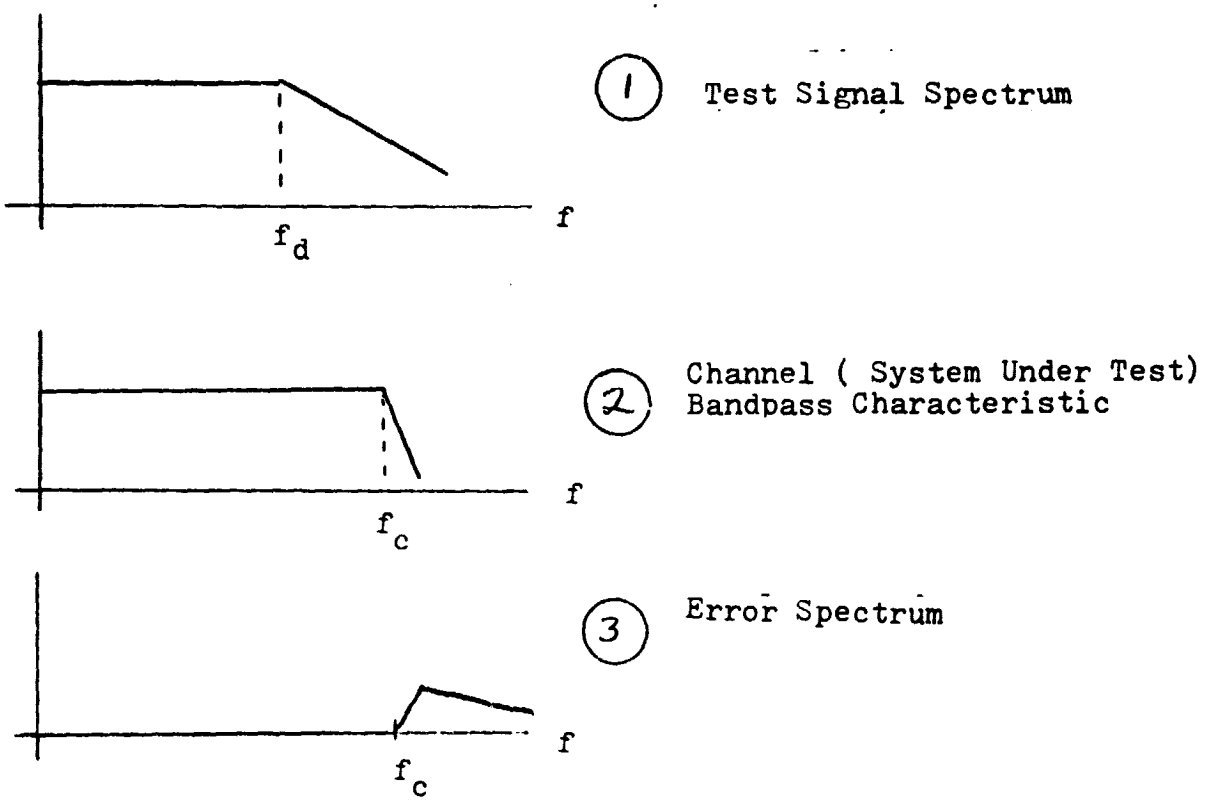

Figure 9 Signal Spectrum Models

$$\text{Test Signal} \quad \begin{cases} 1 : & f \leq f_D \\ 1/(\,1 + jS_D(f-f_D)) : & f > f_D \end{cases}$$

$$\text{Channel Characteristics} \quad \begin{cases} 1 : & f \leq f_D \\ 1/(\,1 + jS_C(f-f_C)) : & f > f_C \end{cases}$$

S_D and S_C are parameters controling the low-pass roll-off rates of the test signal and channel characteristics. This model was selected in order to synthesize the error signal spectrum observed experimentally.

For the model selected, channel distortion occurs for spectral components $f > f_C$. The error signal at point 3, Figure 8, is

$$E(f) = 1/(\,1 + jS_D(f-f_D) - 1/((\,1 + jS_D(f-f_D))(\,1 + jS_C(f-f_C)))$$

and

$$E(f) = (S_C(f-f_C))^2/((\,1-S_CS_D(f-f_D)(f-f_C))^2 + (S_D(f-f_D) + S_C(f-f_C))^2)$$

for $f > f_C$. Figure 10 is an example case of $E(f)$ shown as a function of f.

The next step in this analysis is to characterize the error spectrum as a function of specific PN Test Set parameters such as the reference channel delay adjustment. Figure 11 is a block-diagram of the model utilized for the analysis. Both the PN data spectrum and the system are assumed to be first-order, and described as follows:

PN Data Spectrum: $1/(\,1 + j\,\omega/\omega_d)$

System-Under-Test Transfer Function: $1/(\,1 + j\,\omega/\omega_c)$

where ω_d and ω_c are the data and channel cutoff frequencies respectively.

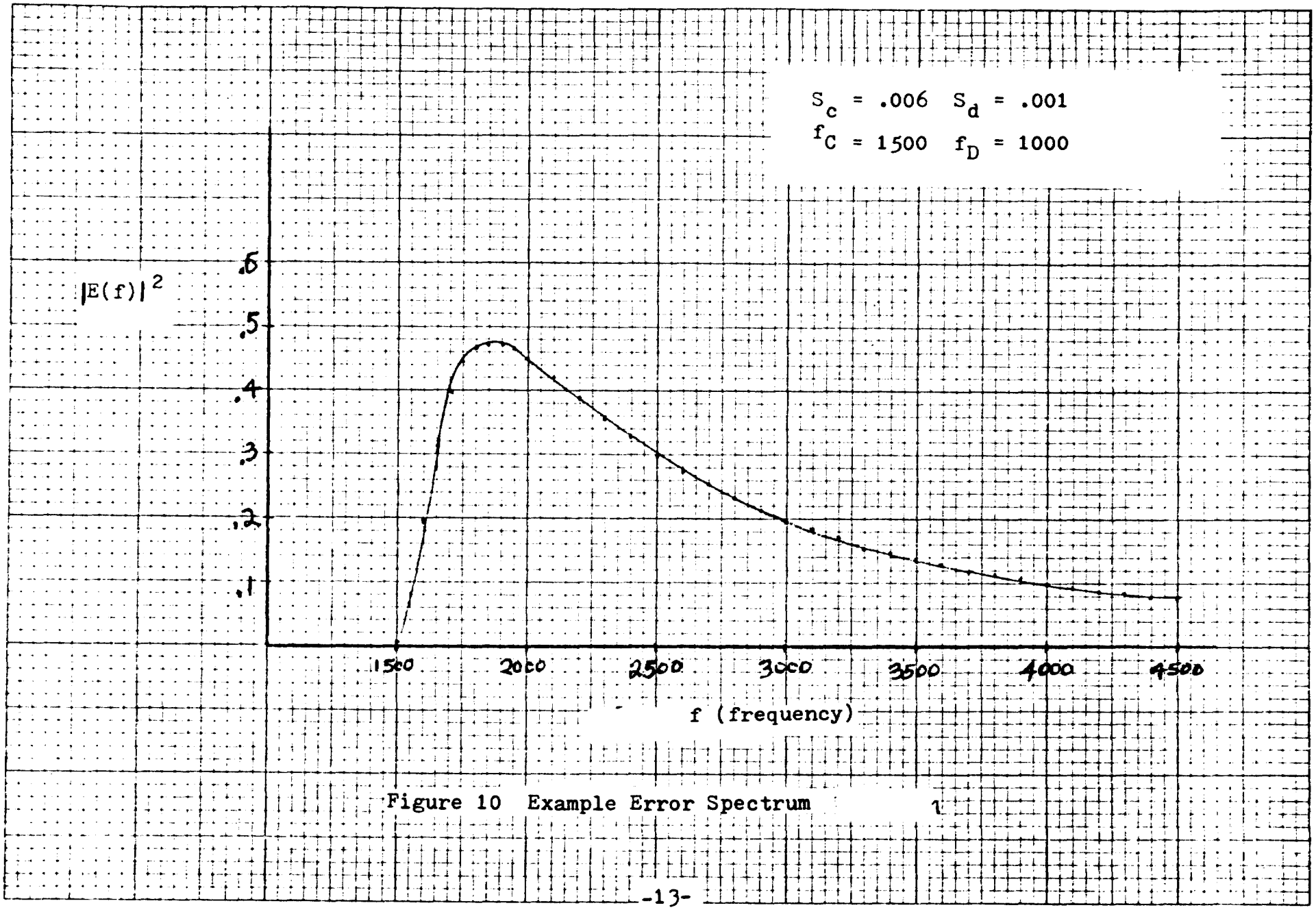

Figure 10 Example Error Spectrum

The delay operation of Figure 11 is characterized by the transfer function: $\epsilon^{-j\tau_D\omega}$

where τ_D is the PN test-set delay adjustment. The reference channel gain adjustment capability of the PN test-set is not modeled in this analysis.

The error spectrum is $|\mathcal{E}(\omega)|^2$, where

$$\mathcal{E}(\omega) = \frac{\epsilon^{-j\tau_D\omega}(1 + j\omega/\omega_c) - 1}{(1 + j\omega/\omega_d)(1 + j\omega/\omega_c)}$$

The normalized mean-square distortion is

$$E_{ms} = \frac{\int_0^\infty |\mathcal{E}(\omega)|^2 d\omega}{\omega_d \pi/2} .$$

$\mathcal{E}(\omega)$ and E_{ms} were calculated as a function of τ_D for the case:

$$f_d = \omega_d/(2\pi) = 1500 \text{ Hz}$$
$$f_c = \omega_c/(2\pi) = 2000 \text{ Hz}$$

and the resusts are shown in Figures 12 and 13.

Figure 12 gives percent mean-square distortion as a function of τ_D. The channel group delay is

$$\tau_{CH}(\omega) = -d\Theta(\omega)/d\omega = \frac{\omega_c}{\omega_c^2 + \omega^2}$$

and at $\omega = 0$, $\tau_{ch} = 79.6\ \mu$ sec. As is seen in Figure 12, minimum percent mean-square distortion occurs for a delay setting considerably less than 79.6 μsec. In fact, the minimum mean-square distortion occurs for $\tau_D \approx 37.5\ \mu$ sec.

Figure 13 shows plots of $\mathcal{E}(\omega) = \mathcal{E}(2\pi f)$ as a function of f (frequency) for several values of τ_D . It is observed that if τ_D is set below 37.5 μsec. , the value that yields minimum mean-square distortion, the error spectrum peaks below f_c. As τ_D is increased, the peak moves up in frequency, is at about f_c for τ_D = 37.5 μsec. , and moves up in frequency rapidly as τ_D increases.

The rapid shift in the error spectrum for delay settings near the setting for minimum distortion can be observed experimentally by monitoring the PN test-set error signal in the frequency domain (spectral analysis) or in the time domain (oscilloscope).

Figures 14, 15, and 16 present an intuitive explanation of the observations. Figure 14 represents the reference signal (B of Figure 11) on a plot showing spectral amplitude, frequency, and delay (τ_D). This plot represents the PN test-set test signal. Figure 15 represents the system-under-test output (A of Figure 11) on the same type plot. Figure 16 shows the reference signal and system-under-test output signal superimposed. As τ_D is adjusted, the reference amplitude spectrum moves parallel to the delay axis of the figure. The minimum rms distortion (minimum rms difference between system output and reference) occurs for a delay setting somewhat less than the system low-frequency group-delay. As can be seen in Figure 16, if τ_D is decreased from its optimum value, the higher frequency components have a better match, however, there is a greater mismatch at lower frequencies. This results in an error spectrum having most of its energy in the lower frequency range. If τ_D is increased above its optimum value, the lower frequency components have a better match, but now the large mismatch occurs at higher frequency.

In summary, the PN test-set error signal spectrum is very dependent on delay setting. If the system under test requires a consideration of error spectrum as well as total rms distortion, it may result that minimum rms distortion is not optimum performance

because of an error spectrum requirement. This suggests the possibility of a filtering operation, to occur after the difference amplifier in the PN test-set, to weight the error spectral components according to the specification or criterion imposed. For example, error above channel cutoff may have a linearly decreasing importance. The possibility of post-difference filtering should be further investigated.

An experiment was performed to verify the analysis of the spectral properties of the PN Test Set error output signal. Referring to Figure 11, the experiment was performed with 2 KHz-third order test data and a low-pass channel as the system under test. Figure 17 is the spectrum of the PN Test Set 2 KHz test signal, and Figure 18 is the spectrum of the output of the system under test. The difference, or error spectrum, is shown in Figure 19, and it is the RMS value of this signal that is measured by the test-set.

As indicated by the analysis, the error spectrum peaks near the cut-off frequency of the data channel under test. The error spectrum of Figure 19 can be compared to the error spectrum calculated from the mathematical model (Figure 10). The agreement between the model and experimental data is fair.

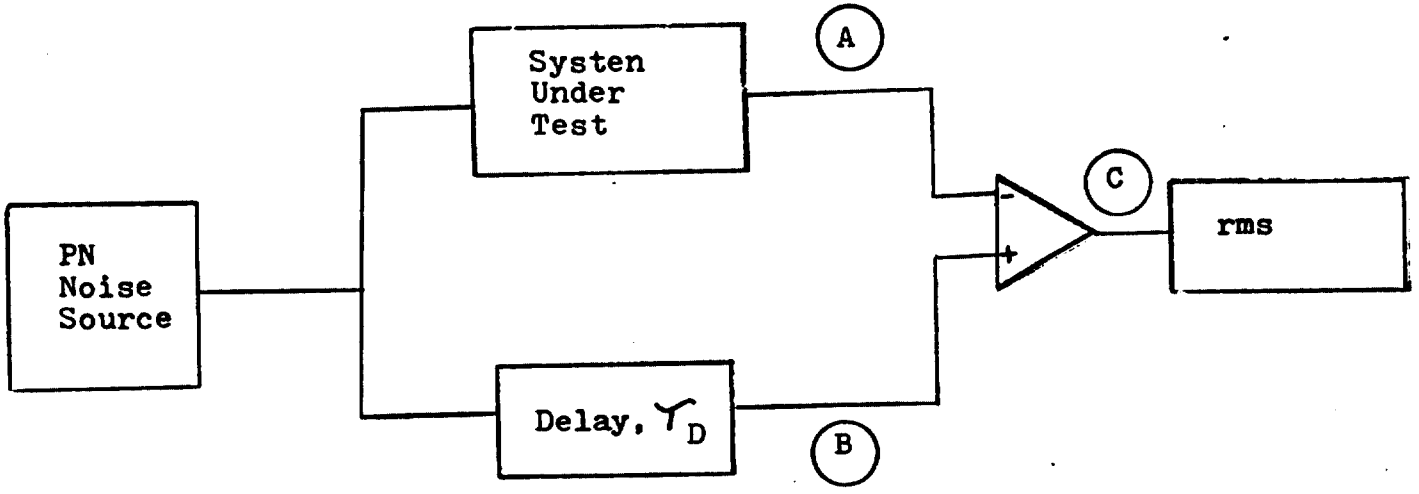

Figure 11 - Model of rms Distortion Measurement

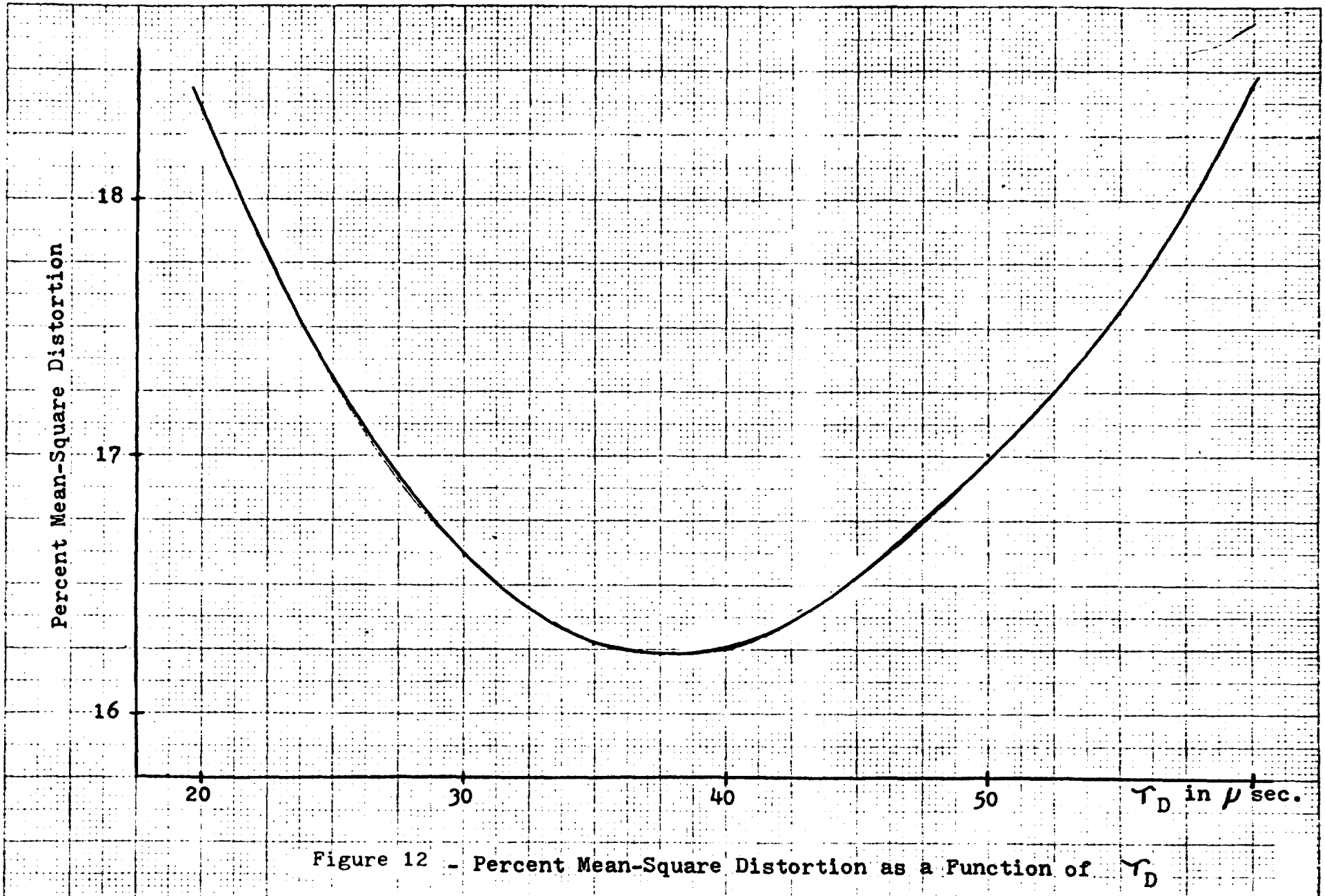

Figure 12 - Percent Mean-Square Distortion as a Function of τ_D

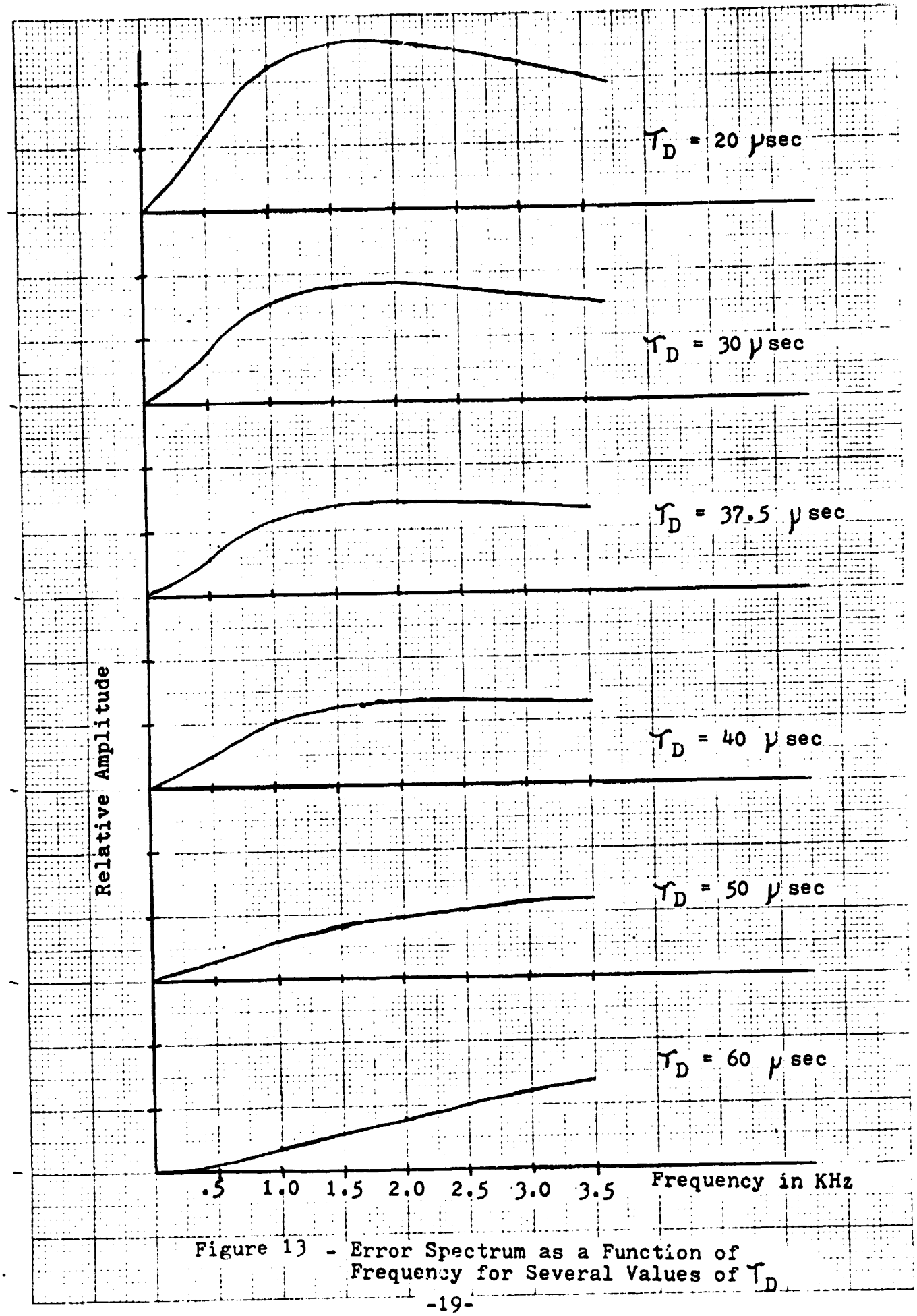

Figure 13 - Error Spectrum as a Function of Frequency for Several Values of τ_D

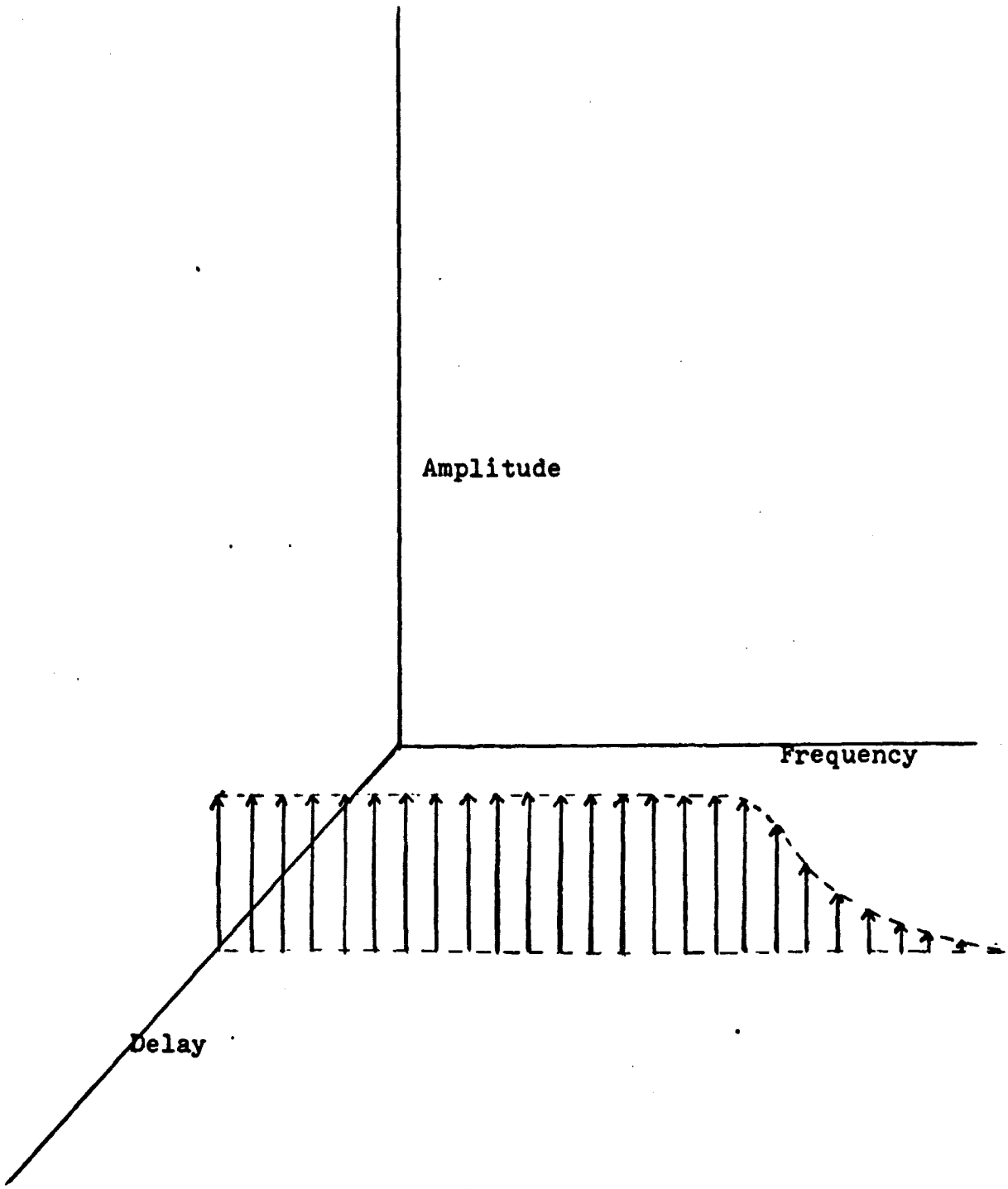

Figure 14 - Reference Signal Spectrum

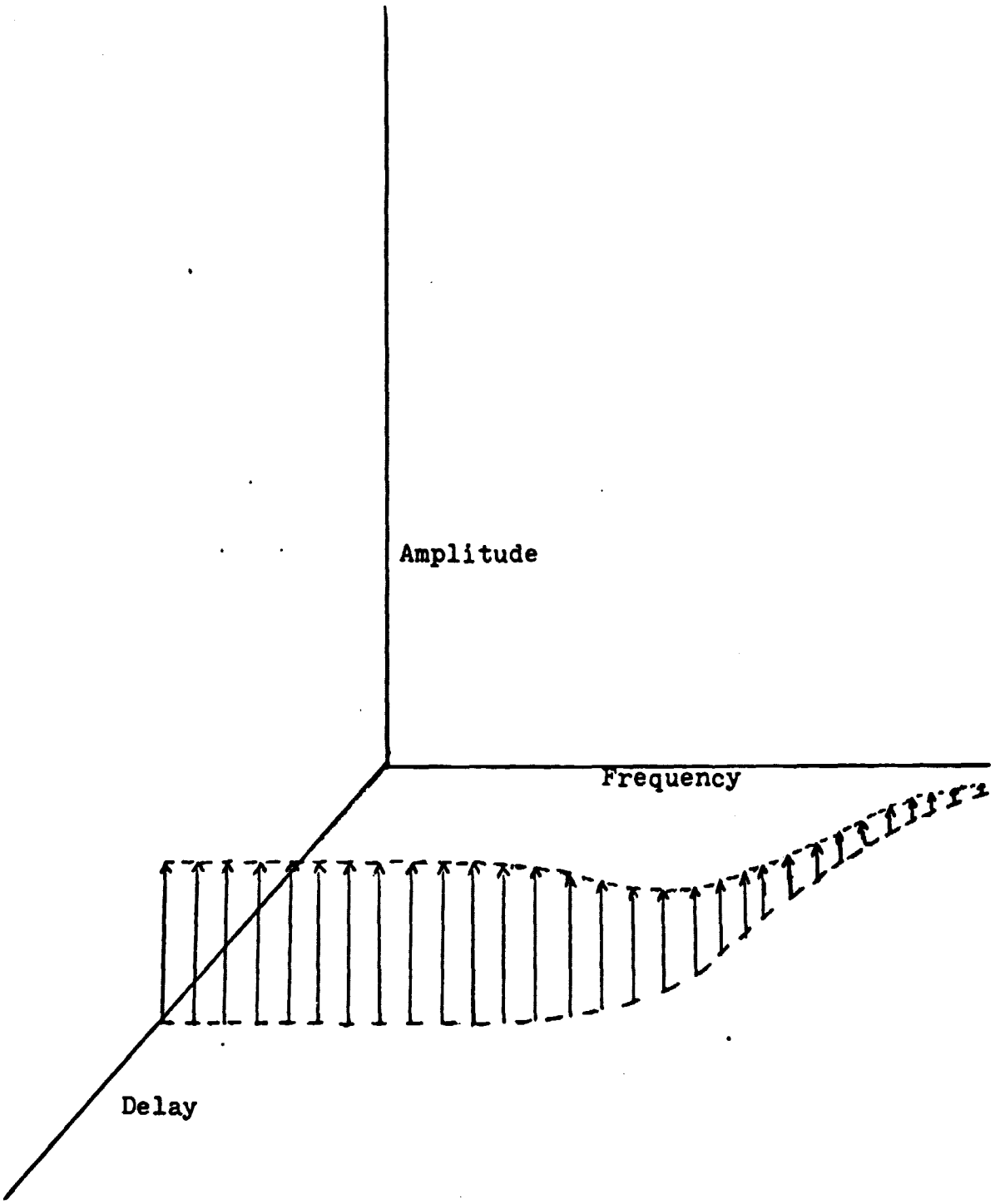

Figure 15 - System-Under-Test Output Spectrum

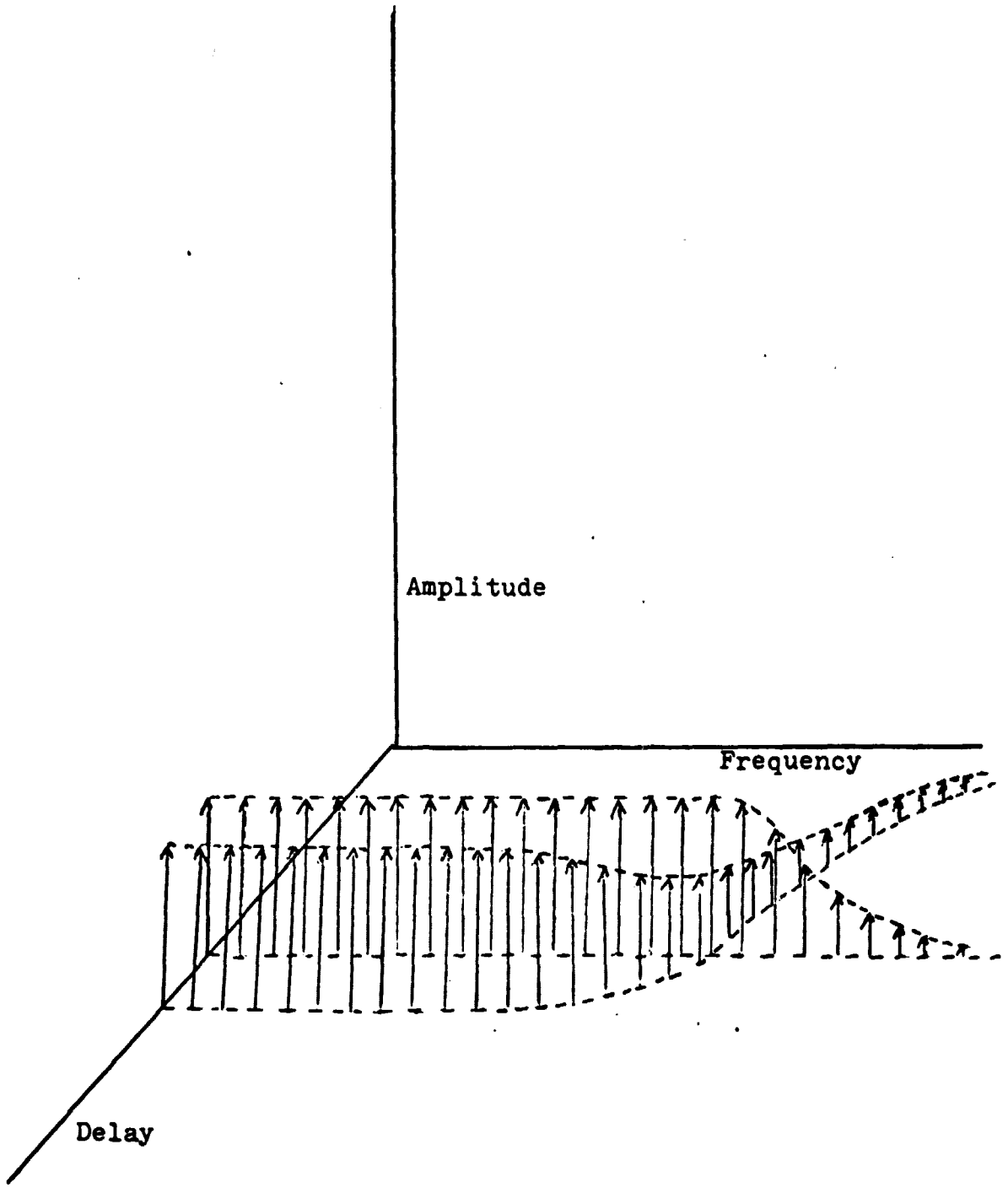

Figure 16 - Composite Difference, PN Test-Set Error Spectrum

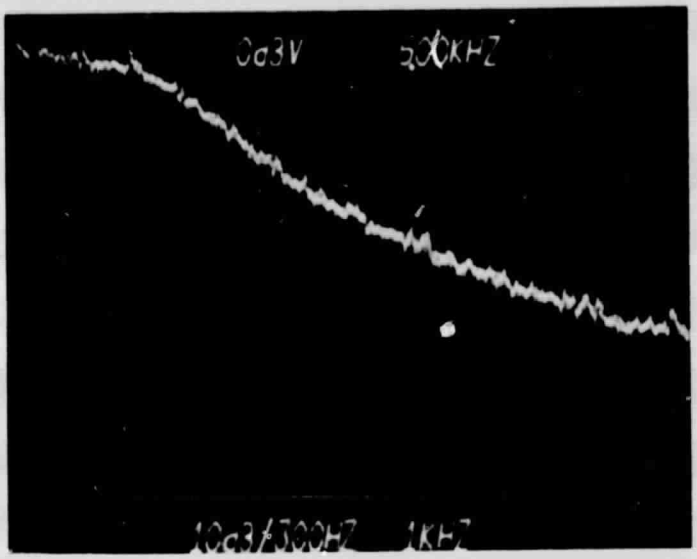

Figure 17 PN Test-Set 2 KHz Test Signal Spectrum

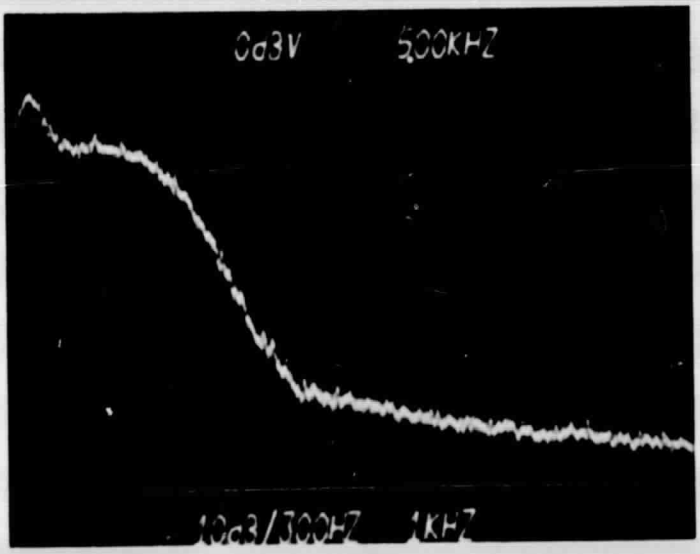

Figure 18 Output Spectrum of the System-Under-Test

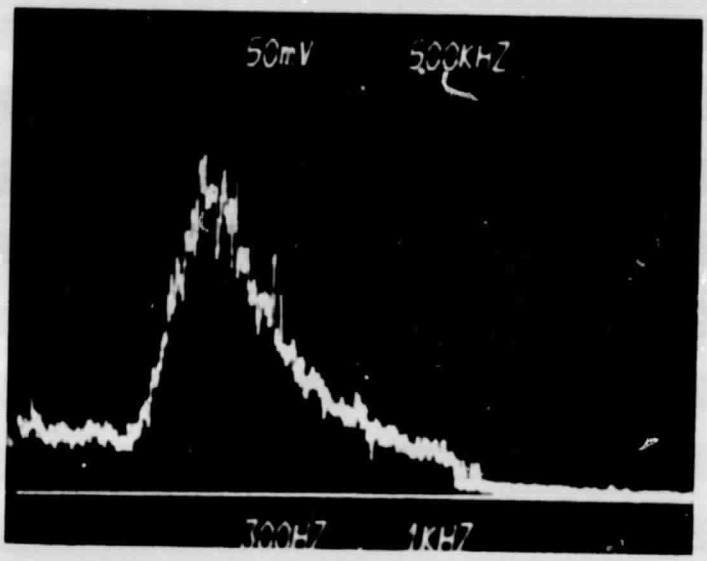

Figure 19 Error Spectrum

2.3 RMS Distortion in a Channel With Uniform Phase Shift

This section reports the results of an analysis which considered the effect of channel phase shift on RMS error as measured by the PN Test-Set. The current test-set design compensates for channel gain and delay in order to make an RMS distortion measurement. It was shown that a modification of the test-set design would allow uniform channel phase-shift to be compensated during the error minimization procedure.

Figure 20 is a block diagram of the current PN Test-Set design. The measurement procedure involves adjusting reference channel gain and delay, compensation for these channel parameters, resulting in a minimization of the RMS value of the difference signal.

From Figure 20, the squared error signal is

$$S_E^2(\omega) = (S_X H - G S_X \epsilon^{-jD\omega})(S_X^* H^* - G S_X^* \epsilon^{jD\omega})$$

If

$$H(\omega) = \epsilon^{-j\phi}$$

then

$$S_E^2(\omega) = |S_X|^2 (1 + G^2 - 2G \cos(D\omega - \phi))$$

IF $\phi = 0$, $\overline{S_E^2}$ (composite RMS distortion) is minimized when G = 1 and D = 0 because $S_E^2(\omega) = 0$ for this condition. However, if $\phi = \pi/2$, no combination of G and D will minimize the composite RMS distortion such that

$$S_E^2(\phi = 0) = S_E^2(\phi = \pi/2).$$

Since uniform phase-shift in a channel can be removed during signal processing, it may be desirable to have the capability to compensate for uniform channel phase-shift

and make the RMS distortion measurement insensitive to this parameter. This capability can be provided by including I (in-phase) and Q (quadrature-phase) reference channels as shown in Figure 21.

With the system of Figure 21, the squared error signal is

$$S_E^2(\omega) = (S_x H - G_I S_x \epsilon^{-jD_I} - jG_Q S_x \epsilon^{-jD_Q})^* (S_x^* H^* - G_I S_x^* \epsilon^{-jD_I} + jG_Q S_x^* \epsilon^{jD_Q})$$

For the case

$$H(\omega) = \epsilon^{j\phi},$$

$$S_E^2(\omega) = |S_x|^2 (\epsilon^{j\phi} - G_I \epsilon^{-jD_I\omega} - jG_Q \epsilon^{-jD_Q\omega})^* (\epsilon^{-j\phi} - G_I \epsilon^{jD_I\omega} + jG_Q \epsilon^{jD_Q\omega}).$$

Now set $D_I = 0$ and $D_Q = 0$, then

$$S_E^2(\omega) = S_x^2 (\epsilon^{j\phi} - G_I - jG_Q)(\epsilon^{-j\phi} - G_I + jG_Q).$$

$\overline{S_E^2(\omega)}$ will be minimized for

$$G_I = \cos(\phi) \quad \text{and} \quad G_Q = \sin(\phi).$$

An argument for making RMS distortion measurements insensitive to uniform channel phase shift is that no channel capacity is lost due to a uniform phase shift, and the original waveform can be recovered by introducing the complement of the channel phase shift as a signal processing operation.

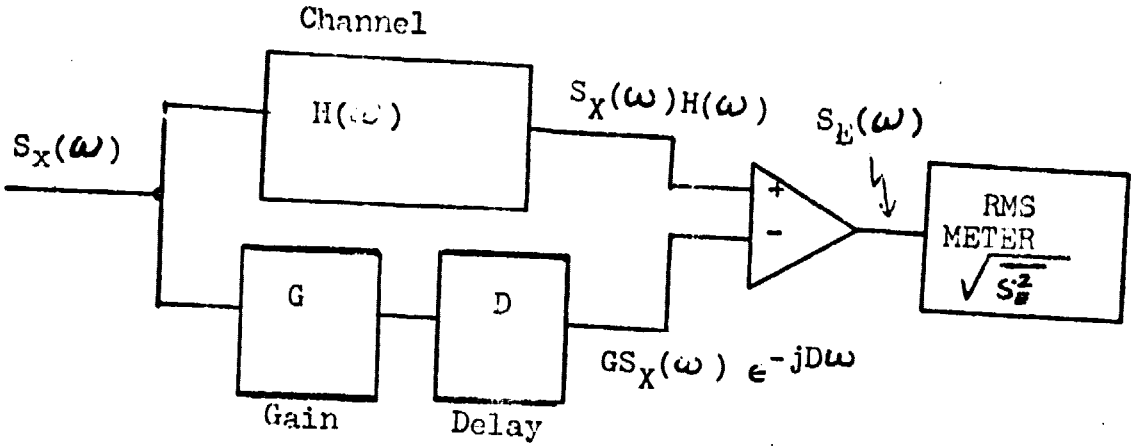

Figure 20 PN Distortion Testing

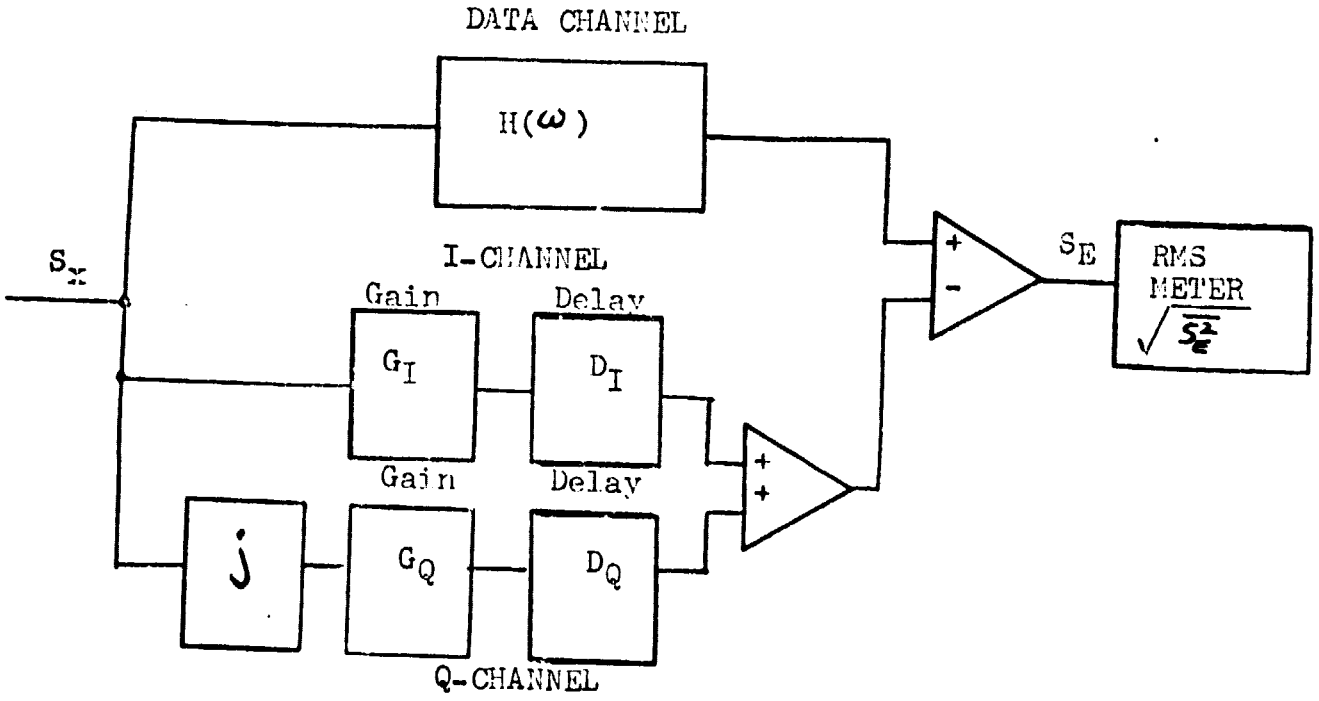

Figure 21 PN Distortion Testing with I and Q Reference Channels

2.4 Television Picture Quality Related to Channel RMS Distortion

This section reports the results of an investigation into the feasibility of relating television picture quality to RMS distortion in the channel as measured by the Pseudo-Noise Test-Set. Television picture quality is somewhat subjective since the degree of tolerence of interference varies amoung viewers. The results of a survey by the Television Allocation Study Organization, which relates average picture grading to signal-to-noise ratio, can be used to relate picture quality to percent RMS distortion. The interference signal used in the survey was random noise, and the results are tabulated in Figure 22.

The block diagram of Figure 23 shows an arrangement for the experimental study of RMS error as measured by the PN Test-Set and channel interference or distortion versus subjective grading of television picture quality.

GRADE	DESCRIPTION	PERCENT RMS DISTORTION ALLOWED FOR GIVEN PERCENT OF VIEWERS		
		25%	50%	75%
Excellent	Extremely High Quality	1.3%	.6%	.3%
Fine	High Quality, Enjoyable Viewing, but Perceptible Interference	3.2%	2.0%	1.3%
Passable	Acceptable Quality, Interference not Objectionable	5.6%	4.5%	3.2%
Marginal	Poor Quality, Interference Somewhat Objectionable	8.9%	7.1%	5.6%
Inferior	Very Poor Quality, Interference Definitely Objectionable	17.8%	14.1%	11.2%
Unuseable	Picture too bad to be Watched	25.1%	20.0%	15.8%

Figure 22 Survey Results Related to RMS Distortion

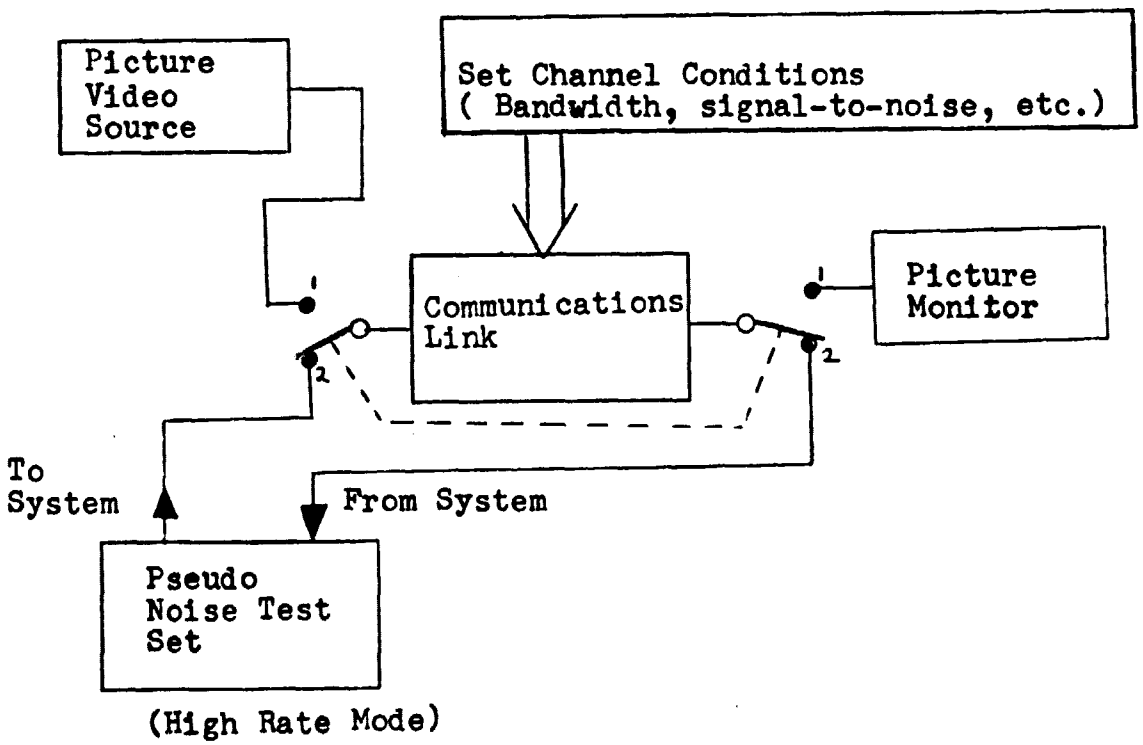

Figure 23 Experimental Arrangement

3. Digital Filter Modification

This section describes a design modification to the PN Test-Set. The objective of the modification is to include a digital filtering capability internal to the unit. The digital filter pair will form the data and reference signals in the "low-rate" data mode of the test-set. The digital filters will operate with the existing system clock, and one of the primary advantages of the unit will be the capability to program the filter parameters by selecting an operating clock frequency in the external-clock mode. The block-diagram of Figure 24 shows the relation of the digital filter pair to the existing test set functional components.

The design is a nonrecursive realization of a finite impulse response filter with twenty delay elements. A Hanning window is applied to improve the filter sidelobe structure.

Effectively, the sampling rate is the PN sequence clock rate. The required delay is provided by two twenty-element delay lines, one each for the data and reference channels. The delay units are 74S74 D-type flip-flops.

The digital filter pair, fabricated on an AUGAT wire-wrap board, includes clock drive units (74S40), the delay lines, Hanning weighting networks, and summing amplifiers. The filters interface with the PN test set main digital board at four points: data clock (1/43.3), data (1/43.6), reference clock (1/43.11), and reference data (1/43.8).

The filter outputs are available in the analog filter bay on BNC connectors. To use the digital filter set, connection is made as follows:

Digital Filter Output	PN Test Set Interface
D	LR1-D
R	LR1-R

The digital filters are twentieth order implementations of a nonrecursive finite impulse filter with Hanning window weighting. The weighting is as follows:

m	a_m
0	0
1	.003
2	.022
3	.076
4	.174
5	.318
6	.495
7	.682
8	.846
9	.960
10	1.000
11	.960
12	.846
13	.682
14	.495
15	.318
16	.174
17	.076
18	.022
19	.003
20	0

The filter response is shown in Figure 25. In the figure, frequency is normalized to the PN test set clock frequency, f_{ck}. The filter cut-off frequency is $.04f_{ck}$ or $f_{ck}/25$. The response is shown in figure 1 for the frequency range

$$0 \leq f/f_{ck} \leq .5 .$$

$f = f_{ck}/2$ corresponding to $f/f_{ck} = .5$ is the folding frequency, and the total filter response is periodic with repetitions at an f_{ck} interval. Figure 26 is a sketch of the filter response in the interval $0 \leq f \leq 1.5\ f_{ck}$, the spectrun on the input PN sequence, and the spectrum of the resulting data waveform.

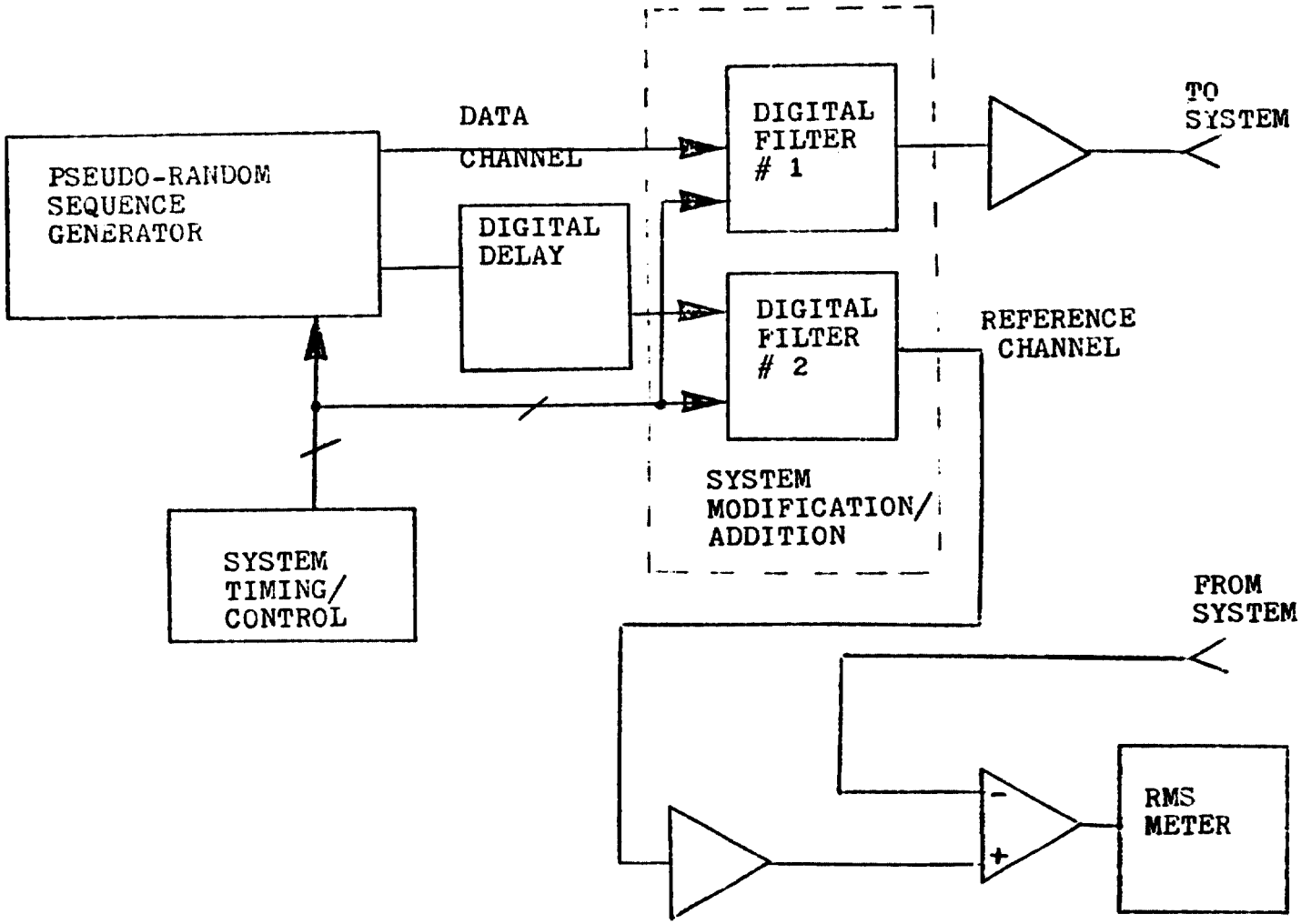

Figure 24 Digital Filter Modification

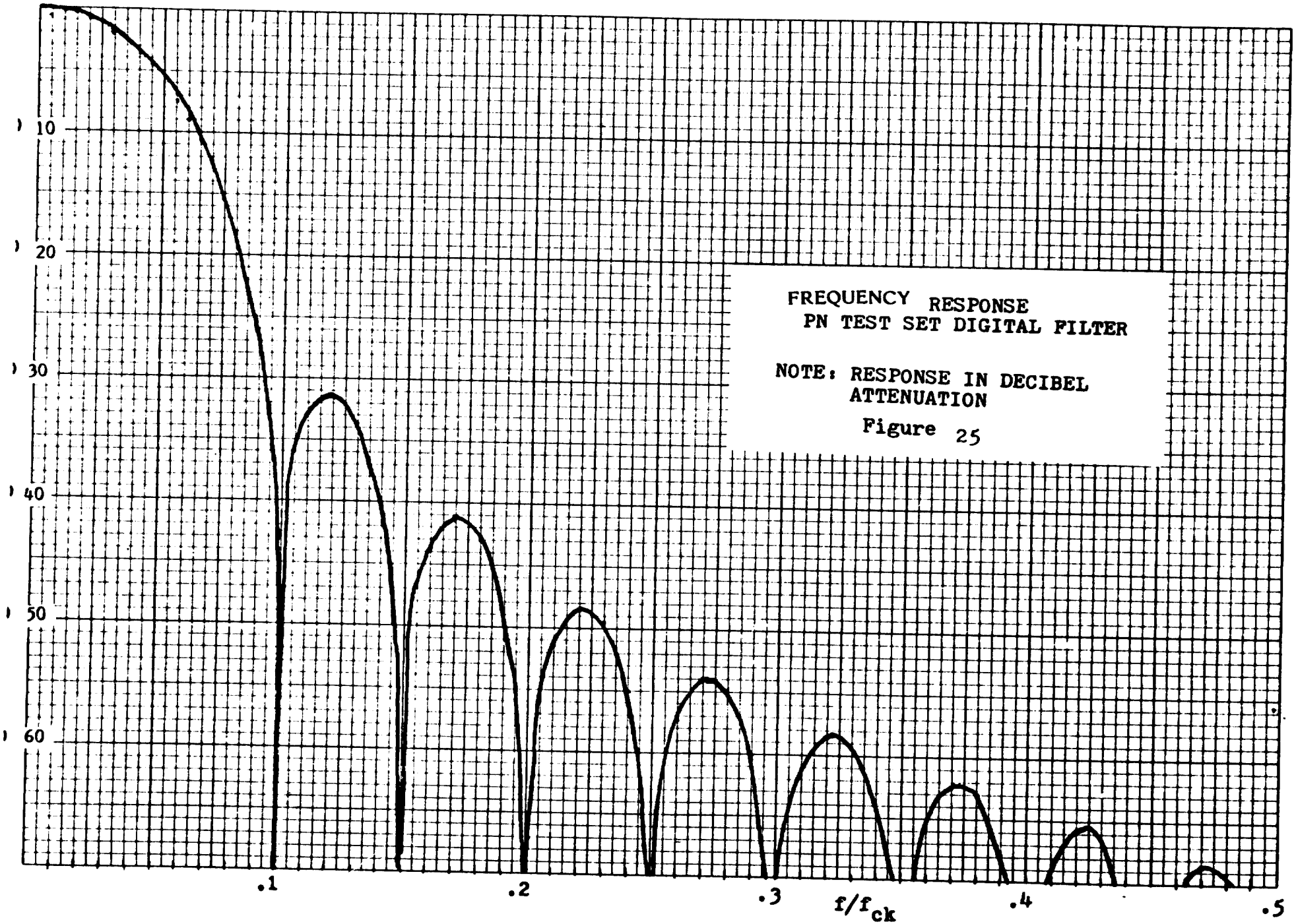

FREQUENCY RESPONSE
PN TEST SET DIGITAL FILTER

NOTE: RESPONSE IN DECIBEL ATTENUATION

Figure 25

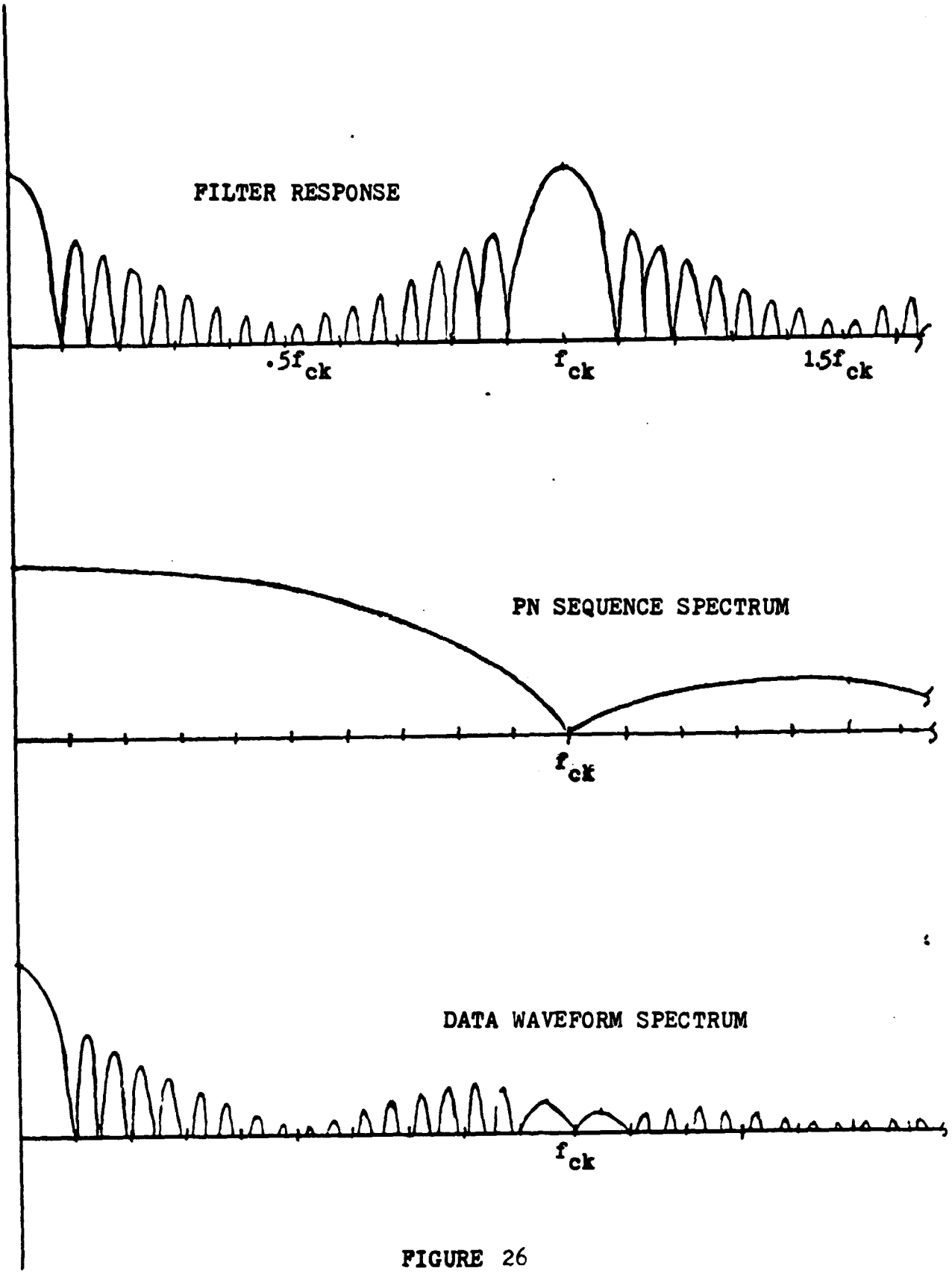
FILTER RESPONSE
.5f ck
f ck
1.5f ck
PN SEQUENCE SPECTRUM
f ck
DATA WAVEFORM SPECTRUM
f ck

FIGURE 26

4. TECHNIQUE FOR FINDING BINARY WORDS FOR OPTIMUM NON-PERIODIC AUTOCORRELATION

Non-Periodic Autocorrelation of a Binary Sequence. The non-periodic autocorrelation of a function (sequence) of binary digits

$$\{a_0, a_1, a_2, \cdots a_{N-1}\}$$

is

$$C(k) = \sum_{i=0}^{N-1-k} a_i \oplus a_{i+k} - (N-k)$$

Optimum Autocorrelation. For a binary sequence, the following is desired.

$$C(k) = \begin{cases} 0, +1, \text{ or } -1 \text{ for } k=1, 2, \ldots N-1 \\ -N \text{ for } k=0 \end{cases}$$

It is known that solutions exist for N=1, 2, 3, 4, 5, 7, 11, and 13. Also, it has been proven that no solutions of odd length exist between N=13 and N=101. This effort investigates a technique for the synthesis of the code with optimum autocorrelation function for a given length N, where optimum means the code with:

$$\text{MIN}|C(k)|, \quad k=1, 2, \ldots N-1.$$

The technique consists of treating any sequence $\{a\}$, except the all zero sequence, as a subsequence of a maximum length sequence. Any sequence $\{a_0, a_1, a_2, \ldots a_{N-1}\}$, except the all zero sequence, is a subsequence of any maximum length sequence of length:

$$L \geq 2^N - 1.$$

Example of the Optimization Technique.

Select Base Code. A simple example will illustrate the basic idea of the synthesis technique. Consider the sequence:

1001011.

This is a maximum length sequence with characteristic polynomial:

$$Z^3 + Z^2 + 1,$$

and will be called the Base Code.

Trinomial Identification with POLTE1. The computer program POLTE1 can be used to find the trinomial that contain the sequence characteristic polynomial as a factor. Trinomials that contain Z^3+Z^2+1 as a factor up to degree 6 are:

$1+Z^2+Z^3$
$1+Z+Z^5$
$1+Z^4+Z^6$

where we include only those trinomials that include the term Z^0.

Location of Optimum Weight Subsequence. The next step is to find subsequences of the maximum length sequence where:

$$N_1-N_0 = 0 \text{ or } \pm 1$$

where N_1 is the number of 1's in the subsequence, and N_0 is the number of 0's. Table 1 shows subsequences of length 1, 2, ... N-1 that satisfy the above condition, along with the relative position of the shifted subsequence.

The relative position for each of the subsequences is calculated with reference to the diagram in Figure 27.

The relative position is the number of shifts right required to move the particular subsequence in $\{a\}$ to the position shown in Figure 1 . Utilizing information obtained from Figure 27, is N_s is the subsequence length;

$$i = N-N_s .$$

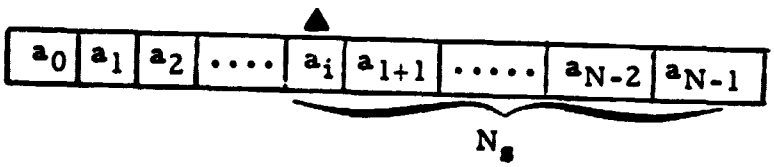

▲ : Subsequence Position (First Bit)

N_s: Subsequence Length

Figure 27

As an example of the calculation of the relative position, consider the subsequence 011100. (N_s equals 6 and i equals 1.)

$\{a\}$: 1 0 0 1 0 1 1 (▽)

Subsequence : 0 1 1 1 0 0 (△)

The required shift from ▽ to △ is 4, as shown in Table 1. As another example, consider the subsequence 1001. (N_s equals 4 and i equals 3.)

$\{a\}$: 1 0 0 1 0 1 1 (▽)

1 0 0 1 (△)

The required shift from ▽ to △ is 3.

Autocorrelation Shift and Subsequence Shift. The next step in the procedure is to indicate the polynomial (trinomial) which indicates phase position for the subsequence generated at each position for the autocorrelation process.

The polynomials (trinomials) are those that contain the sequence characteristic polynomial as a factor, as determined by POLTE1. The particular polynomial for a given autocorrelation shift is chosen from the group so that the power of the second term (exponent) is equal to the autocorrelation shift. The result of this procedure is shown in Table 2.

Subsequence Relative Position for Cyclic Shifts of Base Code. The next step in the procedure is to form a table that includes all possible codes generated by shifts in the basic code, and the relative positions of the subsequences that have the desired weights. In our example,

1 0 0 1 0 1 1

is the Base Code.

1 0 1 1 1 0 0

is another code generated by shifting the phase of the Base Code. For a Base Code of length N, there are N different codes, which will have different auto-correlation (non-periodic) functions.

Subsequence Length	Subsequence	Weight	Relative Position
6	110010	0	2
	100101	0	1
	001011	0	0
	011100	0	4
5	11100	1	4
	11001	1	3
	10010	-1	2
	00101	-1	1
	01011	1	0
	01110	1	5
4	1100	0	4
	1001	0	3
	0101	0	1
3	110	1	5
	100	-1	4
	001	-1	3
	010	-1	2
	101	1	1
	011	1	0
2	10	0	2
	10	0	5
	01	0	3
	01	0	1
1	1	1	6
	1	1	3
	1	1	1
	1	1	0
	0	-1	5
	0	-1	4
	0	-1	2

Table 1 Subsequences (1, 2, ... N-1) and Corresponding Relative Position

Autocorrelation Shift	Subsequence Length	Polynomial	Subsequence Shift
1	6	$1+Z+Z^5$	5
2	5	$1+Z^2+Z^3$	3
3	4	$1+Z^2+Z^3$	2
4	3	$1+Z^4+Z^6$	6
5	2	$1+Z+Z^5$	1
6	1	$1+Z^4+Z^6$	4

Table 2 Polynomials Containing Second Terms Equal to the Autocorrelation Shift

Matching Subsequence Relative Position to Subsequence Shift.

The next step is to identify in each column of Table 2 those subsequence relative positions that correspond to the subsequence shift as identified in Table 2 and listed in Table 3. Table 4 is the result of this operation where the matching condition is indicated by the circles.

The matching condition means that the autocorrelation function (non-periodic) will have the weight indicated for that row for the indicated shift. For example, from Table 4 , code 1110010 (Base Code 1001011 shifted 5 places) will have non-periodic autocorrelation -7, 0, 1, 0, 1, 0, 1 as shown below:

```
1110010
1110010
-------
0000000      : -7

1110010
 1110010
 -------
 001011      :  0

1110010
  1110010
  -------
  01110      :  1

1110010
   1110010
   -------
   1100      :  0

1110010
    1110010
    -------
    101      :  1

1110010
     1110010
     -------
     01      :  0

1110010
      1110010
      -------
      1      :  1
```

As another example, consider the code 1011100 (Base code 1001011 shifted 3 places). From Table 4 , the non-periodic auto correlation is:

-7, 1, ___, -1, 0, 1.

Subsequence			Subsequence Relative Position for Phase Shift of Base Code						
Length	Shift	Weight	0	1	2	3	4	5	6
		0	2	3	4	5	6	0	1
6	5	0	1	2	3	4	5	6	0
		0	0	1	2	3	4	5	6
		0	4	5	6	0	1	2	3
		1	4	5	6	0	1	2	3
		1	3	4	5	6	0	1	2
5	3	-1	2	3	4	5	6	0	1
		-1	1	2	3	4	5	6	0
		1	0	1	2	3	4	5	6
		1	5	6	0	1	2	3	4
		0	4	5	6	0	1	2	3
4	2	0	3	4	5	6	0	1	2
		0	1	2	3	4	5	6	0
		1	5	6	0	1	2	3	4
		-1	4	5	6	0	1	2	3
3	6	-1	3	4	5	6	0	1	2
		-1	2	3	4	5	6	0	1
		1	1	2	3	4	5	6	0
		1	0	1	2	3	4	5	6
		0	2	3	4	5	6	0	1
2	1	0	5	6	0	1	2	3	4
		0	3	4	5	6	0	1	2
		0	1	2	3	4	5	6	0
		1	6	0	1	2	3	4	5
1	4	1	3	4	5	6	0	1	2
		1	1	2	3	4	5	6	0
		1	0	1	2	3	4	5	6
		-1	5	6	0	1	2	3	4
		-1	4	5	6	0	1	2	3
		-1	2	3	4	5	6	0	1

Table 3 Subsequence Relative Positions for Phase Shifts of Base Code

Subsequence			Subsequence Relative Position for Phase Shift of Base Code						
Length	Shift	Weight	0	1	2	3	4	5	6
6	5	0	2	3	4	⑤	6	0	1
		0	1	2	3	4	⑤	6	0
		0	0	1	2	3	4	⑤	6
		0	4	⑤	6	0	1	2	3
5	3	1	4	5	6	0	1	2	③
		1	③	4	5	6	0	1	2
		-1	2	③	4	5	6	0	1
		-1	1	2	③	4	5	6	0
		1	0	1	2	③	4	5	6
		1	5	6	0	1	2	③	4
4	2	0	4	5	6	0	1	②	3
		0	3	4	5	6	0	1	②
		0	1	②	3	4	5	6	0
3	6	1	5	⑥	0	1	2	3	4
		-1	4	5	⑥	0	1	2	3
		-1	3	4	5	⑥	0	1	2
		-1	2	3	4	5	⑥	0	1
		1	1	2	3	4	5	⑥	0
		1	0	1	2	3	4	5	⑥
2	1	0	2	3	4	5	6	0	①
		0	5	6	0	①	2	3	4
		0	3	4	5	6	0	①	2
		0	①	2	3	4	5	6	0
1	4	1	6	0	1	2	3	④	5
		1	3	④	5	6	0	1	2
		1	1	2	3	④	5	6	0
		1	0	1	2	3	④	5	6
		-1	5	6	0	1	2	3	④
		-1	④	5	6	0	1	2	3
		-1	2	3	④	5	6	0	1

Table 4 Identification of Matching Relative Positions and Corresponding Subsequent Shifts

Since there is no result for 3 shifts (match for 3) shown in Table 4, the sidelobe will not be 0, -1, or 1. This result in confirmed by direct calculation of the non-periodic autocorrelation.

Finding Optimum Words of Length Less Than the Base Code Length. As was shown, the code word 1110010 has ideal non-periodic autocorrelation. This was indicated in Table 4 by a match in the "5" column for each subsequence length. The same 7-bit maximum length basic sequence can be used for finding optimum words that have length less than 7 and are subsequences of the basic ML code. For example, consider all 5-bit subsequences of 1001011.

In considering such a task, a modification of Table 4 , encompassing changes to the "Shifts" and "Subsequence Relative Positions" columns is beneficial. This is shown in Table 5 . Subsequence lengths of 4 and less are analyzed due to the exploration of strictly 5-bit codes. Numbers in Table 4 are shifted by: 7-5 = 2 places. Numbers in the "Shift" column are shifted down two places for Table 5 , while numbers in the "Subsequence Relative Position" columns are shifted right two places.

Table 5 indicates that code 10111 will have non-periodic autocorrelation (-5, 0, -1, 0, -1). The code 10111 is the initial 5-bit subsequence of the basic code 1001011 shifted by 3. This result is confirmed below:

```
10111
10111
-----
00000        : -5

10111
 10111
------
 1100        :  0

10111
  10111
-------
  010        : -1

10111
   10111
--------
   01        :  0

10111
    10111
---------
    0        : -1
```

Subsequence			Subsequence Relative Position for Phase Shift of Base Code						
Length	Shift	Weight	0	1	2	3	4	5	6
4	5	0	2	3	4	(5)	6	0	1
		0	1	2	3	4	(5)	6	0
		0	6	0	1	2	3	4	(5)
3	3	1	(3)	4	5	6	0	1	2
		-1	2	(3)	4	5	6	0	1
		-1	1	2	(3)	4	5	6	0
		-1	0	1	2	(3)	4	5	6
		1	6	0	1	2	(3)	4	5
		1	5	6	0	1	2	(3)	4
2	2	0	0	1	(2)	3	4	5	6
		0	3	4	5	6	0	1	(2)
		0	1	(2)	3	4	5	6	0
		0	6	0	1	(2)	3	4	5
1	6	1	4	5	(6)	0	1	2	3
		1	1	2	3	4	5	(6)	0
		1	(6)	0	1	2	3	4	5
		1	5	(6)	0	1	2	3	4
		-1	3	4	5	(6)	0	1	2
		-1	2	3	4	5	(6)	0	1
		-1	0	1	2	3	4	5	(6)

Table 5 Relative Position Table for Evaluation of 5-bit Subsequences of 7-bit Base Code

Generalization of the Optimization Technique. In general, utilization of the techniques described with an ML sequence of length L makes possible location of all optimum code words of length N where:

$$L \geq 2^N - 1$$

For the example given, L = 7 and N = 3. However, location of optimum code words of length 7 and 5 was completed and possibly location of others of length N could have been completed such that:

$$L < 2^N - 1$$

It is possible for a given ML code (length L) to find optimum words of up to length L with this technique. However location of all optimum words of length N where $L \geq 2^N - 1$ is guaranteed. This is quaranteed due to the fact an L bit sequence (ML) will have all possible N bit sequences, except the all zero sequence if $L \geq 2^N - 1$.

The generalization of the procedure to consider sidelobe values other than 0, +1, and -1 would involve considering subsequences of other weights. The most general table would include all possible subsequence weights.

Improved Table for Finding Subsequence Shift and Relative Position Match. Table 4 can be compressed by using the results of column "0" to calculate the column in which a match with the shift parameter occurs for each subsequence. The calculated value is:

Match Column = (Shift - relative position for 0 Phase Shift) Mod L

Table 6 is the resulting table, where an obtained code word is identified when one value appears in each group of calculated match column. As shown, Table 5 indicates that an optimum 7-bit code results if the Base Code is shifted five places.

Summary of the Optimization Technique. In summary, the list of steps below describes the operations necessary for the optimization technique.

- Step 1:

  Select code length, ℓ (input), then select an ML code of order N, $L = 2^N - 1 \geq \ell$ called the Base Code.

Subsequence			Calculated	Common in All Groups	
Length	Shift	Weight	Match Column	Through Group 1	Group
		0	3	3	
6	5	0	4	4	1
		0	5	5	
		0	1	1	
		1	6		
		1	0		
5	3	-1	1	1	2
		-1	2		
		1	3	3	
		1	5	5	
		0	5	5	
4	2	0	6		3
		0	1	1	
		1	1	1	
		-1	2		
3	6	-1	3		4
		-1	4		
		1	5	5	
		1	6		
		0	6		
	1	0	3		5
2		0	5	5	
		0	0		
		1	5	5	
1	4	1	1		
		1	3		6
		1	4		
		-1	6		
		-1	0		
		-1	2		

Table 6 Improved Table for Finding Subsequence Shift and Relative Position Match

- Step 2:

  Find trinomials that contain the sequence characteristic polynomial (use POLTE1), form Table 2.

- Step 3:

  Search for specific weight subsequences in Base Code, form Table 1.

- Step 4:

  Using the method of Table 6 for each subsequence length of the Base Code, calculate the phase shift of the Base Code required for a match between the shift parameter and the relative position.

- Step 5:

  For all groups in Table 6 find common elements.